frontiers | Frontiers in Earth Science

TYPE Original Research
PUBLISHED 03 November 2022
DOI 10.3389/feart.2022.987731



OPEN ACCESS

EDITED BY
Nicola Alessandro Pino,
Vesuvius Observatory (INGV), Italy

REVIEWED BY
Paolo Galli,
Dipartimento della Protezione Civile, Italy
Spyridon Mavroulis,
National and Kapodistrian University of Athens, Greece
Federica Ferrarini,
G d'Annunzio University of Chieti and Pescara, Italy

*CORRESPONDENCE
Luigi Cucci,
luigi.cucci@ingv.it

SPECIALTY SECTION
This article was submitted to Solid Earth Geophysics, a section of the journal Frontiers in Earth Science

RECEIVED 06 July 2022
ACCEPTED 21 September 2022
PUBLISHED 03 November 2022

CITATION
Cucci L (2022), NW-dipping versus SE-dipping causative faults of the 1783 M7.1 Southern Calabria (Italy) earthquake: The contribution from the analysis of the coseismic hydrological changes.
*Front. Earth Sci.* 10:987731.
doi: 10.3389/feart.2022.987731



# NW-dipping versus SE-dipping causative faults of the 1783 M7.1 Southern Calabria (Italy) earthquake: The contribution from the analysis of the coseismic hydrological changes

Luigi Cucci *

Istituto Nazionale di Geofisica e Vulcanologia, Sezione di Sismologia e Tettonofisica, Rome, Italy

The 1783 Mw7.1 Southern Calabria (Italy) earthquake originated a remarkable number of observations of hydrological changes (variations of flow in springs and streams, liquefaction, changes in water temperature) that occurred in different localities. To provide further constraints on the mechanism and the geometry of the causative fault of the event, I compared the distribution of the hydrological changes with the coseismic strain produced by eight seismogenic sources proposed for the earthquake. The most important outcomes of the study can be summarized as follows: a) the group of potential sources that display the best agreement between expected deformation and hydrological signature consists of NW-dipping systems of three to four surface-rupturing almost pure normal fault segments (Cittanova fault system), capable of generating earthquakes of magnitude Mw6.9–7.1; b) the distribution of the observed coseismic hydrological anomalies does not support the role of the SE-dipping faults as potential sources of the 1783 earthquake; c) the pattern of deformation associated with the best fit source strengthens the hypothesis that the 20 km-long surface ruptures testified soon after the 1783 event reflect primary faulting; d) a minimum magnitude Mw6.9–7.0 is required to obtain the pattern and the extent of distribution of the coseismic hydrological changes observed in the field; e) the location of the hydrological variations that were observed only along the western side of southern Calabria suggests that the Cittanova fault system acts as a hydrological barrier that hampers the groundwater circulation toward the East.

KEYWORDS

**Calabria (southern Italy), 1783 earthquake, coseismic hydrological changes, seismogenic source, static strain**

## 1 Introduction

The seismic history of the Italian Peninsula is punctuated by the occurrence of several large magnitude (M≈7) earthquakes and long-lasting seismic sequences that often heavily affected and hampered the economy and the development of the struck region (e.g. Janku et al., 2012; Galadini, 2022). Field observations and seismological data routinely provide robust constraints about the location, geometry and kinematics of those events that occurred in the last tens of years. On the contrary, the identification of an earthquake source can turn to be a difficult or even controversial task for events that occurred in historical times, even in the presence of historical reports that provide an accurate record of the most destructive earthquakes that occurred over almost twenty centuries in Italy (Rovida et al., 2021). In particular, the narrow strip of land of the Calabria region (the tip of the Italian 'boot') concentrates one fourth of the largest (M≥6) Italian earthquakes (Rovida et al., 2021), yet the full knowledge is lacking about the location and the geometry of the seismogenic source for some of these seismic events. The reasons for these uncertainties stem from a complex geological structure concentrated in a relatively small region; within the general frame of active extension that backs the different interpretations of the investigators, it can happen that two visions confront each other about the characteristics of the seismic source. A paradigmatic case is represented by the 5 February 1783 Mw7.1 earthquake. This earthquake ranks among the largest seismic events ever occurred in Italy and gave rise to the most disastrous sequence in the seismic

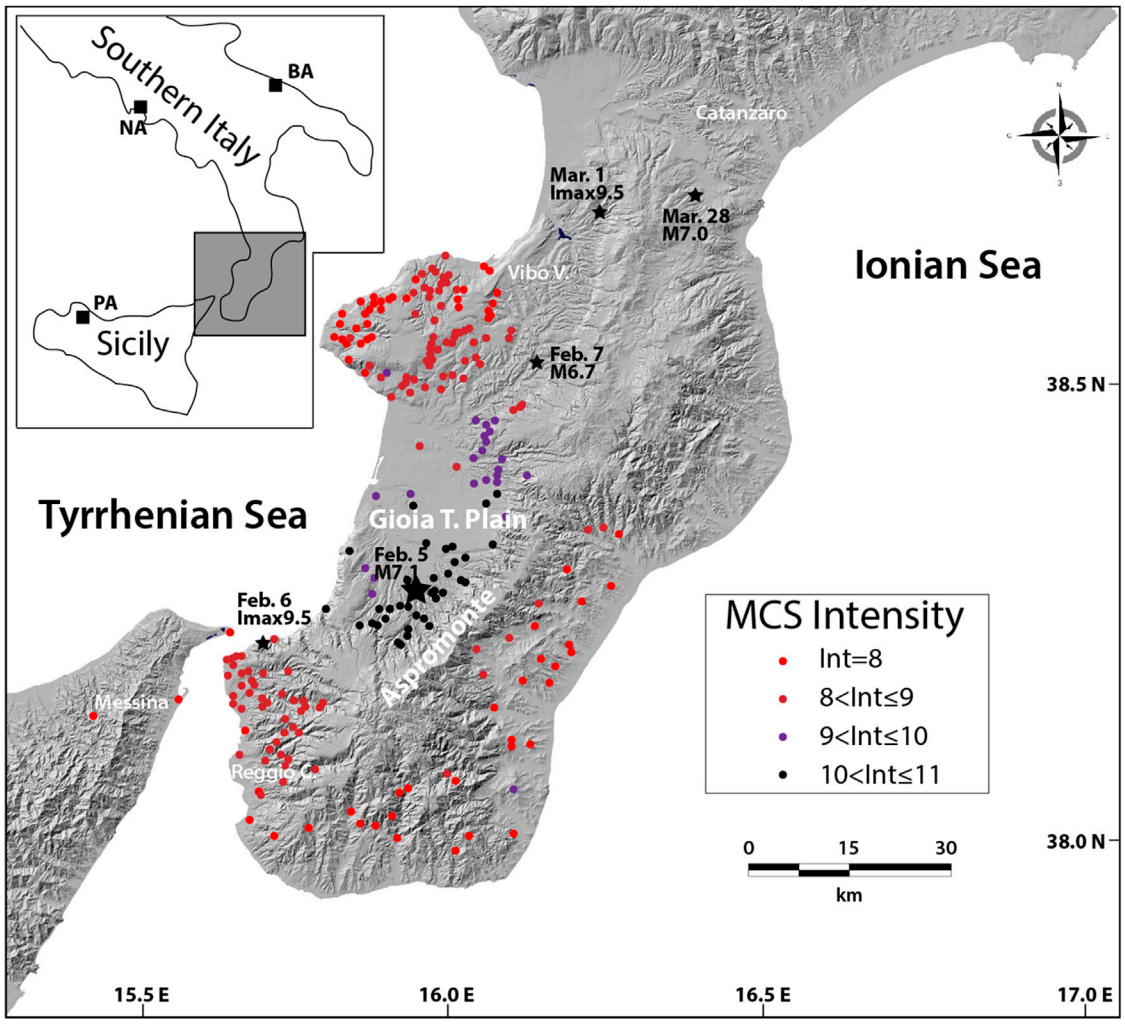


FIGURE 1
Map of the highest MCS intensities (Int>8; Rovida et al., 2021) associated with the 5 February 1783 earthquake. The epicenter of the event is marked by a large black star. The map also shows (with small black stars) the location of the four most powerful earthquakes that occurred during the 1783 seismic sequence. Key for the main towns in the inset:BA, Bari; NA, Naples; PA Palermo.

history of the Peninsula, with other four Mw6-7 earthquakes (Rovida et al., 2021; Locati et al., 2022), over the following 50 days (Figure 1). Most of the investigators ascribe the 5 February event to the activity of NW-dipping, high-angle normal faults, while a second group of researchers contend that the primary seismogenic source is a blind, low-angle normal fault that dips to the E-SE (see References in the section dedicated to the sources of the 1783 earthquake). As the two confronting systems of seismic sources of the 1783 event are compatible with the same stress field and are hardly distinguishable from intensity reports alone, other approaches to infer information would provide improved constraints and opportunity to discriminate among the different interpretations. A possible contribution in this direction is provided by the study of the coseismic hydrological changes originated by the 1783 event, that can be explained by the coseismic static strain and pore pressure changes predicted by the poroelastic theory proposed by Wakita (1975).

Therefore, in this paper I will focus on the hydrological coseismic changes induced by the 1783 earthquake through: 1) the description of the dataset of hydrological data observed after the event; 2) the calculation of the coseismic strain field associated with all the competing potential sources proposed by the investigators and (3) the identification of the source/s that better matches the observed hydrological effects and the other pieces of evidence collected.

## 2 Overview on the 5 February 1783 event

The 5 February 1783 earthquake is one of the largest seismic event ever occurred in peninsular Italy during the last 500 years (a period that coincides with the historical completeness of the seismic catalog for the largest classes of magnitude in Southern Italy, see Stucchi et al., 2004). This $I_0$11 MCS, Mw7.1 earthquake (Rovida et al., 2021), is still remembered more than two centuries later as the "Grande Flagello" (huge scourge) because of the massive destruction that it caused over a territory of 3000 km$^2$ (almost doubled after the damages inflicted by the following large events of the sequence). In particular, the 5 February event struck the Tyrrhenian side of central-southern Calabria and was felt over Sicily and most of Southern Italy (Figure 1); it killed about

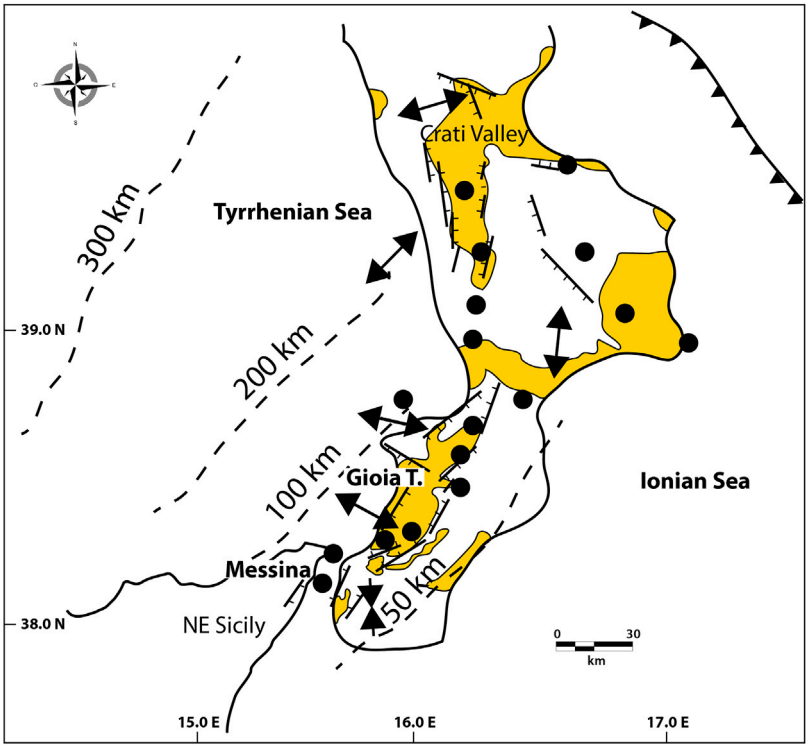


FIGURE 2
Structural and kinematic sketch of the Calabrian Arc. Horizontal strain-rate modified after Faccenna et al. (2014) (Converging black arrows, compressional mean rate; diverging black arrows, extensional mean rate). Solid black line with triangles indicates the present-day wedge front of the Arc. Quaternary continental and marine deposits are shown in yellow. Black circles indicate the epicenters of M>6 earthquakes from the Catalogo Parametrico dei Terremoti Italiani (Rovida et al., 2021). Solid lines indicate the main faults from DISS Working Group (2021) and from ITHACA Working group (2019); barbs indicate the downthrown side. Dashed lines show the isobaths of the top of the Ionian slab from Galli and Peronace (2015).

30.000 people, and more than 130 villages and towns suffered I≥9 MCS (heavy destruction). The 1783 event aroused a huge interest in the European scientific community. An unusual number of scientists, travelers, and technicians, on behalf of the Bourbon government or driven by personal reasons, traveled to the stricken area in the aftermath of the event, to investigate the cause of the earthquake and document its effects (see Table 2 for References). All of them were impressed by the remarkable changes to the landscape, and reported their observations in several monographs, letters, and official reports. This is the reason why the data concerning the environmental effects produced by the 1783 earthquake represents the most extensive record among the historical earthquakes of the past millennium in Italy (Guidoboni et al., 2019 and references therein). The most outstanding primary and secondary effects comprise a 18–20 km-long surface fracture, thousands of landslides with consequent lake damming, subsidence, a moderate tsunami, and widespread hydrological changes.

## 3 Seismogenic sources proposed for the 1783 earthquake

The narrow Calabria region is the onshore part of a wide accretionary wedge called Calabrian Arc (Figure 2). The Arc is the southernmost part of the Southern Apennines, a thrust and fold belt formed above a W-dipping subduction zone that retreated eastward since Neogene (Malinverno and Ryan, 1986; Faccenna et al., 2001). In particular, the Calabrian Arc is the only region of residual active subduction of Ionian oceanic crust underneath the southern margin of the European plate (Chiarabba et al., 2008). In this geodynamic context, extension developed on the Tyrrhenian side of the upper plate, parallel to the Arc and on top of the subduction. The main normal faulting system runs onshore, and most of the investigators agree that it extends for the entire length of the Arc, between the Crati Valley to the North and the North-Eastern Sicily to the South, and that it originated the largest Calabrian earthquakes (cfr the literature cited in DISS Working Group, 2021 and in ITHACA Working Group, 2019). Nevertheless, a debate still exists about the characteristics of the faults responsible for the largest earthquakes that occurred in this area, especially in its southern portion, and in particular about the location and the geometry of the 5 February 1783 earthquake causative fault.

### 3.1 NW-verging earthquake sources

Several studies (Cotecchia et al., 1986; Westaway, 1992; Tortorici et al., 1995) consider the Gioia Tauro Plain, that is the 1783 epicentral area where most of the effects concentrated, as a Graben structure with the master fault on its eastern flank at the border with the Aspromonte Massif. The investigators refer to that fault as the Cittanova Fault (Cotecchia et al., 1986; Tortorici et al. 1995; Galli and Bosi, 2002). Evidence of the surface expression of a potential source at this location was witnessed and accurately described in the aftermath of the earthquake by De Dolomieu (1784), who reported a 18–20 km-long, ~1 m-wide surface fracture separating the metamorphic rocks of the Massif from the continental successions and the sedimentary marine terrains of the Plain. Similar, independent descriptions of this surface feature were reported also by several other coeval investigators (Coccia, 1783; De Leone, 1783; Sarconi, 1784; Caristina, 1786; Vivenzio, 1788). Cotecchia et al. (1986) were the first to hypothesize that this NW-facing scarp could be the surficial expression of the 1783 earthquake fault. This interpretation was later on supported by geological (Tortorici et al. 1995), geophysical (Jacques et al., 2001) and paleoseismological (Galli and Bosi, 2002; Galli and Peronace, 2015; for the relationship with the adjacent source of the February 7 event see also Galli et al., 2007) studies. In summary, the 25–30 km-long, 60–70°-dipping, surface breaking Cittanova Fault accounts for the interpretation of the investigators who favor a NW-facing 1783 earthquake fault. Further considerations regarding the relationships between the morphotectonic pattern of the Gioia Tauro Plain, the 1783 epicentral location, and the distribution of the damage, led some of the Authors to assume that other fault strands which characterize the landscape of the basin could be involved in the 1783 rupture process along with the Cittanova Fault. This is the case of the sources proposed by Galli and Bosi (2002) and by Jacques et al. (2001), that are both composed of additional fault segments North (Polistena or Galatro Faults) and South-West (S. Eufemia Fault) of the Cittanova Fault. Finally, I will also consider three other NW-dipping seismogenic sources that were associated with the 1783 event on the basis of different approaches. The first one is from Valentini et al. (2017), who presented a probabilistic hazard model and proposed a ~60 km-long structure including two other fault segments that extend South of the Cittanova Fault and reach the Messina Straits area. The second one is based on magnetic data and modeling and is the ~40 km-long source proposed by Minelli et al. (2016), named Cittanova-Aspromonte Fault, which partly matches the Cittanova Fault and extends southward within the Aspromonte Massif. The last source, that is inferred from the inversion of intensity data (code Boxer 4.1 by Gasperini et al., 2010), is a ~50 km-long blind pure normal fault that coincides with the barycentre of the area of the largest earthquake effects. Because there is no constraint for the dip direction of this kind of source, I will consider two alternative seismogenic structures characterized by the same location and opposite sense of dip (towards the NW and the SE). Figure 3 and Table 1 summarize the NW-verging earthquake sources.

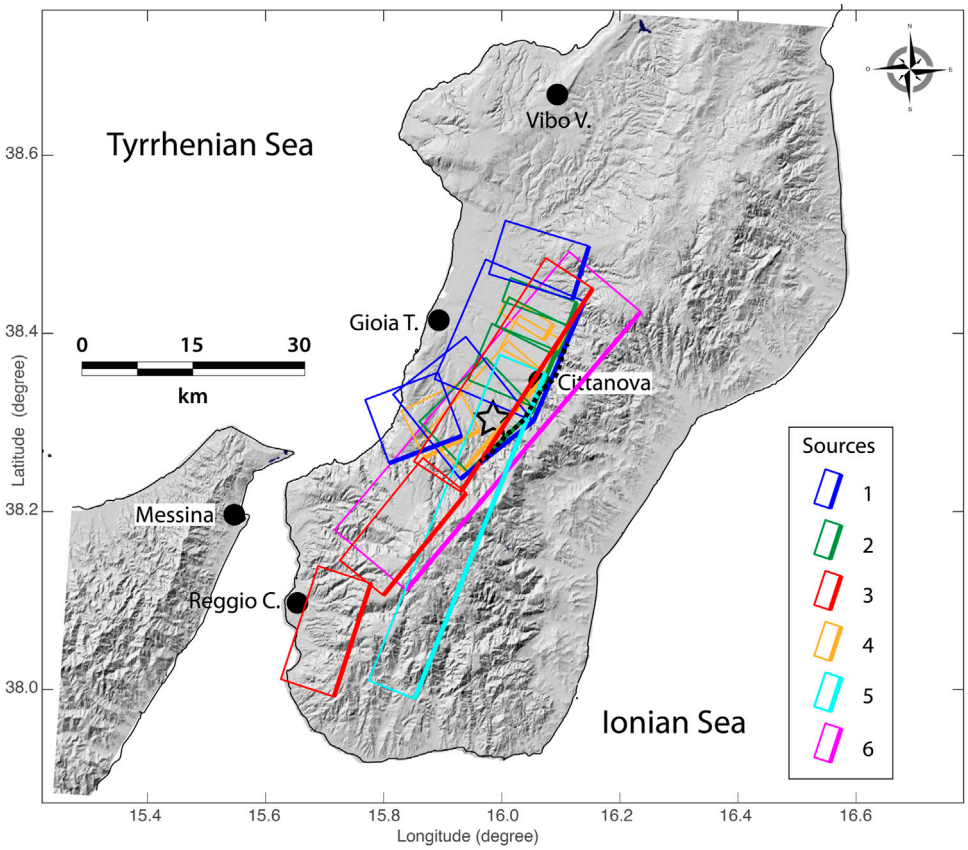


FIGURE 3
Location of the NW-verging competing potentian sources of the 1783 earthquake (epicenter shown as a black star): 1, Jacques; 2, Galli_ Peronace; 3, Valentini; 4,GAlli_Bosi; 5, Minelli; 6, Boxer_NW. A thicker line indicates the top edge of the source. The black dashed line marks the pattern of the surface ruptures observed in the field after the event.

## 3.2 SE-verging earthquake sources

A second group of investigators maintain that the present tectonic activity in the study area is dominated by the Gioia Tauro Fault, a blind, low-angle (30°), ESE-dipping pure normal fault located close to the coast. This interpretation, firstly put forward by Ricchetti and Ricchetti (1991) on the basis of stratigraphic indications, later on was supported by Valensise and D'Addezio (1994) and Tiberti et al. (2017), who claimed the shortage of geological evidence of post early Pleistocene activity along any NW-dipping source in this area. These latter authors called the joint analysis of landscape features, the sediment attitudes and the displacement field predicted by dislocation modeling to support their interpretation. Finally, Pizzino et al. (2004) provided further evidence favoring the Gioia Tauro Fault on the basis of important geochemical anomalies located at the northwestern end of the source. The Gioia Tauro Fault is the seismogenic source associated with the 5 February event into the Database of Individual Seismogenic Sources (DISS Working Group 2021), and shares the same seismotectonic pattern (blind, low-angle, ~East-dipping) of all the major sources proposed in the DISS along the Tyrrhenian side of the Central-Southern Calabrian Arc. In summary, the source envisioned by the DISS is a 25 km-long, 15 km-wide, 30°-dipping fault with the leading edge set at 3 km depth, and capable of generating a Mw 6.6 event. Figure 4 and Table 1 summarize the SE-verging earthquake sources.

# 4 The hydrological signature of earthquake strain

The coseismic hydrological effects have long been observed and witnessed, as they are outstanding phenomena that can be noticed over great distances. In the last decades, several papers (see Cucci 2019 and references therein for a detailed description) provided evidence that some coseismic hydrological changes can be explained by the coseismic static strain and pore pressure changes predicted

TABLE 1 List of the 8 potential sources of the 1783 earthquake that represent the input to the modelling of the coseismic static strain. The names of the single fault segments belonging to a fault system are indicated in italic. The fault parameters not explicitly indicated by the authors are inferred from the empirical relationships by Hanks and Kanamori (1979), Wells & Coppersmith (1994), or from geometric relationships and are indicated in italic. The moment magnitude Mw has been recalculated from the seismic moment associated with each segment.

| Source | | Length (km) | Width (km) | Min Depth (km) | Max Depth (km) | Strike (°) | Dip (°) | Rake (°) | Slip (m) | Mw | Seismic Moment (dyne-cm) | References |
|---|---|---|---|---|---|---|---|---|---|---|---|---|
| Valentini | *Cittanova* | 30 | 14.3 | 0.0 | 13.0 | 213 | 65 | -90 | *2* | 6.9 | 2.6e+26 | Valentini et al. (2017) |
| | *Delianuova* | 19 | 14.3 | 0.0 | 13.0 | 219 | 65 | -90 | *2* | 6.8 | 1.6e+26 | |
| | *Armo* | 14 | 15 | 0.0 | 13.0 | 198 | 60 | -90 | *2* | 6.7 | 1.3e+26 | |
| Minelli | | 43 | 15 | 2 | 16 | 205 | 70 | -90 | 2 | 7.0 | 3.9e+26 | Minelli et al. (2016) |
| Jacques | *Galatro* | 6 | 22 | 0.0 | 20 | 200 | 65 | -95 | 0.9 | 6.3 | 3.6e+25 | Jacques et al. (2001) |
| | *Cittanova_N* | 17 | 23 | 0.0 | 20 | 207 | 60 | -90 | 2.5 | 6.9 | 2.9e+26 | |
| | *Cittanova_S* | 13 | 23 | 0.0 | 20 | 233 | 60 | -90 | 2.5 | 6.9 | 2.2e+26 | |
| | *S. Eufemia* | 11 | 21 | 0.0 | 20 | 250 | 70 | -75 | 1.7 | 6.7 | 1.2e+26 | |
| Galli_Peronace | *Fault1* | 3 | *15* | 0.0 | 13 | 204 | 60 | -90 | 1.9 | 6.2 | 2.6e+25 | Galli and Peronace (2015) |
| | *Fault2* | 5 | *15* | 0.0 | 13 | 214 | 60 | -90 | 1.9 | 6.4 | 4.3e+25 | |
| | *Fault3* | 8 | *15* | 0.0 | 13 | 207 | 60 | -90 | 1.9 | 6.5 | 6.8e+25 | |
| | *Fault4* | 13 | *15* | 0.0 | 13 | 230 | 60 | -90 | 1.9 | 6.7 | 1.1e+26 | |
| Galli_Bosi | *Polistena* | 2.5 | 13 | 0.0 | 11.8 | 212 | 65 | -90 | 0.7 | 5.8 | 5.5e+24 | Galli and Bosi (2002) |
| | *S. Giorgio* | 4.5 | 13 | 0.0 | 11.8 | 210 | 65 | -90 | 0.7 | 5.9 | 8.2e+24 | |
| | *Cittanova* | 17.5 | 13 | 0.0 | 11.8 | 221 | 65 | -90 | 0.7 | 6.4 | 4.1e+25 | |
| | *S. Eufemia North* | 7 | 13 | 0.0 | 11.8 | 244 | 65 | -90 | 0.7 | 6.2 | 1.9e+25 | |
| DISS | | 25.0 | 15.0 | 3 | 10.5 | 30 | 30 | -90 | 0.86 | 6.6 | 9.7e+25 | DISS Working Group (2021) |
| Boxer_SE | | 49.4 | 17.1 | 2 | 14 | 37 | 45 | -90 | 1.5 | 7.0 | 3.8e+26 | Gasperini et al. (2010) |
| Boxer_NW | | 49.4 | 17.1 | 2 | 14 | 217 | 45 | -90 | 1.5 | 7.0 | 3.8e+26 | Gasperini et al. (2010) |

by the poroelastic theory, firstly put forward by Wakita (1975). Under this theory, the coseismic strain field caused by an earthquake produces dilatation or contraction of the rocks; the consequent opening or closing of saturated cracks leads to decrease or increase in the groundwater discharge of streams and springs. The amplitude of the hydrological changes is proportional to the volumetric strain field; thus, an increase of the groundwater discharge will theoretically occur in contractional areas and a decrease in extensional areas. A discharge increase is expected following the compressional strain changes caused by the displacement on a 60°-dipping normal fault, which is the most frequent type of seismogenic source in the Southern Apennines (DISS Working Group, 2021; ITHACA Working Group, 2019). This issue potentially provides critical constraints to the style of faulting of major historical earthquakes that produced large and documented amounts of hydrological effects. Research in this direction has been carried out on modern and ancient earthquakes, mostly on normal faulting events (Grecksch et al. 1999; Montgomery and Manga, 2003; Tertulliani and Cucci, 2009; Cucci and Tertulliani, 2015; Petitta et al., 2018; Cucci, 2019). In most cases, the models of coseismic static strain accounted for the hydrological signatures of the styles of faulting and for the geographical reach of the hydrological response.

## 5 The 1783 coseismic hydrological effects

The coseismic hydrological effects ascribed to the 5 February mainshock compose a remarkable set of data (Figure 5).

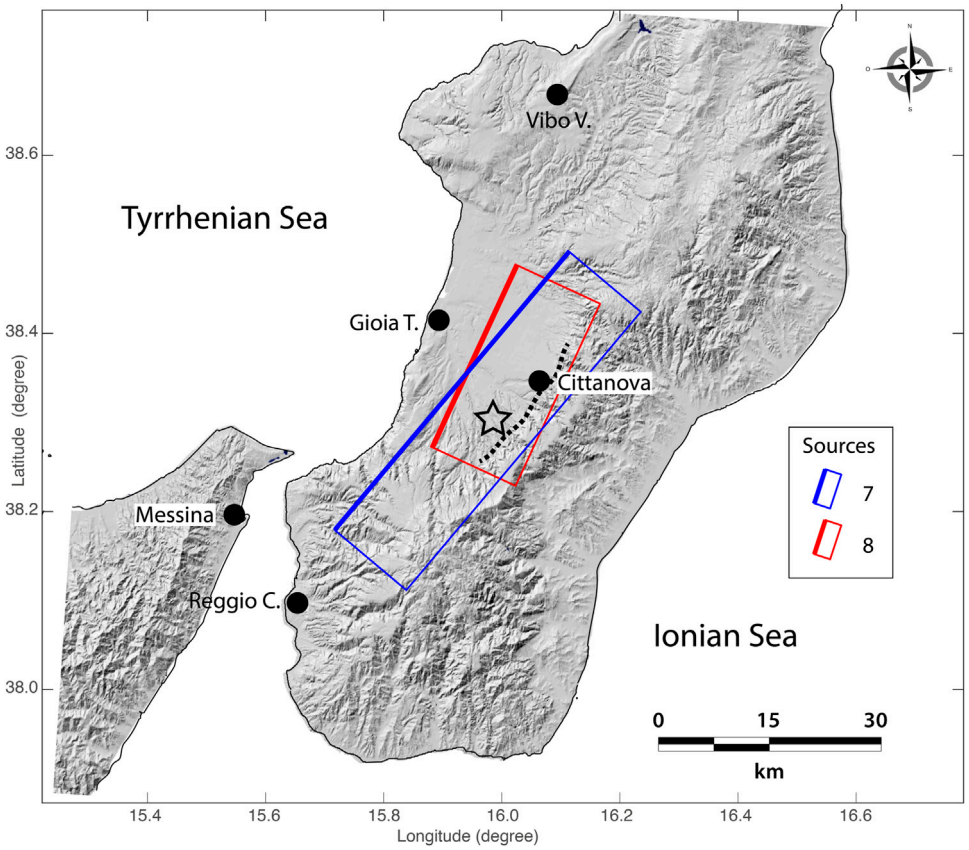


FIGURE 4
Location of the SE-verging competing potentian sources of the 1783 earthquake (epicenter shown as a black star): Boxer_SE; 8, DISS. A thicker line indicates the top egde of the source. The black dashed line marks the pattern of the surface ruptures observed in the field after the event.

Hydrological changes were observed over a wide area between 1 and 112 km from the macroseismic epicenter and comprise (i) increase (most of the data) or decrease of the discharge of streamflows, springs and water level in wells, (ii) liquefaction, (iii) turbid flow from rivers and springs, (iv) chemical-physical variations in the temperature and composition of the waters. Although the liquefaction usually occurs within subsurface sediments, some indications suggest a deeper mechanism of generation (Cox et al., 2012; Montgomery and Manga, 2003; Montgomery et al., 2003). Then I include liquefaction as one of the mechanisms that contribute to the increase of flow.

The reports about the coseismic hydrological changes were consistent among the coeval investigators. The core of the information concerning the hydrological changes comes from detailed "travel diaries" by Vivenzio (1783 and 1788) and by Sarconi (1784), sent in the epicentral area on behalf of the Kingdom of Naples. In particular, the latter report is accompanied by an appendix of 67 engravings, mostly made by P. Schiantarelli (an architect member of the mission headed by M. Sarconi), that faithfully document the occurrence of the effects; examples of these coeval drawings are reported in Galli (2000) and some are shown in Figure 6.

Each observation has been accurately reconsidered and localized cross-checking the original description with topographic maps at different scale (1:10.000, https://geoportale.regione.calabria.it; 1:25.000, https://www.igmi.org/) for the recognition of the toponyms. Also, the re-reading of the extensive literature available made it possible to increase (records n. 13, 32, and 62 are novel points from a coeval source, see Table 2) the total number of records in the dataset, which now counts 78 observations relative to 53 different localities. Table 2 displays the hydrological changes reported after the 5 February 1783 earthquake. Based on the reliability of each reference/account, I assigned a threefold quality code (A/B/C) to the data. The best rank 'A' is assigned to the observations that were clearly described and consistently reported by coeval investigators; second and third ranking is given to observations not clearly described or with tenuous evidence ('B'), or mislocated and/or hardly associated with

the event ('C'). The factors that can influence the assessment of the quality of a hydrological observation are basically of two different types. First, the pattern of change in the streamflow and spring discharge is characteristic, as it tends to peak hours or few days after the earthquake and then it gradually declines to return to the pre-earthquake conditions during a longer period (months and even years). The coeval sources consistently report this behaviour for most of the springs and streams following the 1783 earthquake. Second, climatic factors such as rainfall can originate hydrological observations that are not associated with coseismic crustal strain. A very light and limited rainfall is reported by Vivenzio (1788) in the area of Monteleone (presently Vibo Valentia) in the early morning of February 5; consequently, as a precaution I excluded from the calculations of coseismic strain the hydrological observations located within 15 km from this place (records n. 13, n. 15, n. 30, see Table 2). Finally, some geomorphological features can locally alterate the course of streamflows, i.e., the 1783 earthquake caused a great number of superficial effects such as hundreds of landslides damming valleys upstream, and/or displacements locally blocking springs, like the records n. 35 and n. 54, that were discounted as well. For a complete review about the bias and caveats that can affect the data selection see Cucci (2019). Following the assessment of the data quality, 63 hydrological observations (37 relative to liquefaction, 26 to spring/streamflow increase/decrease or to generic emission of water) obtained rank 'A' and were included in the calculations of the coseismic strain; other 15 observations, ranked 'B' or 'C', were excluded.

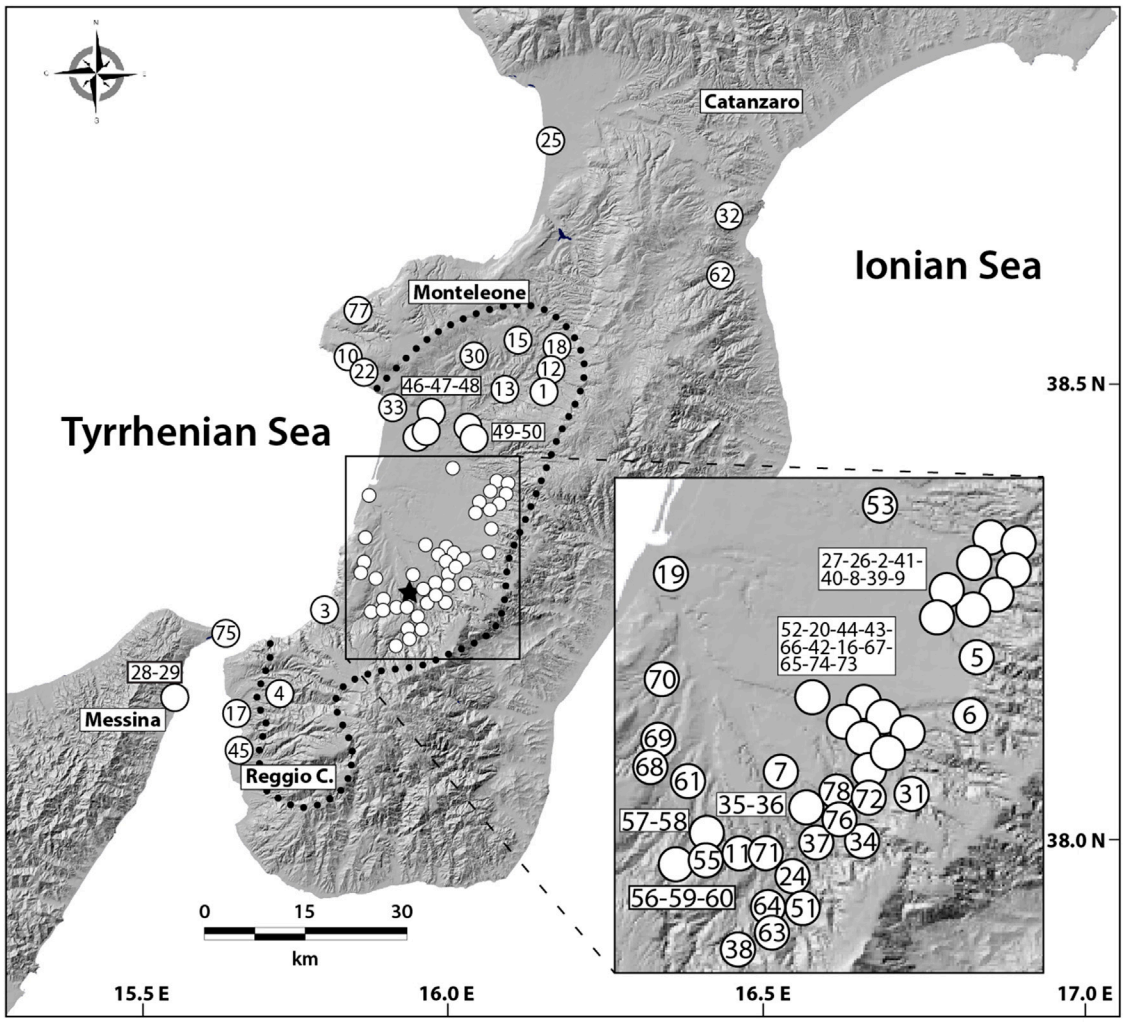


FIGURE 5
Distribution of the hydrological anomalies (white circles) associated with the 5 February 1783 earthquake. Numbers inside the circles correspond to the records in Table 2. Observation n. 21 is located outside the map. Dotted line encloses the area of heavy destruction (Int>9 MCS). A black sar marks the location of the epicenter of the event.

## 6 Calculations of strain

I compared the plots of coseismic strain to the distribution of the 63 rank 'A' coseismic hydrological variations, to provide constraints to the geometry and the location of the earthquake faults; the main goal is to single out a preferred fault or, alternatively, to exclude some of the sources put forward by the investigators. This approach assumes that the streamflow changes are the response to coseismic strain variations (Muir-Wood and King, 1993), so I expect to find an increase of discharge in areas affected by compression and a decrease in areas affected by dilatation. The static strain change was calculated using a fault dislocation model in an elastic half-space with uniform isotropic elastic properties following Okada (1985), with the code Coulomb 3.4 (Toda et al., 2011). The outputs of these computations are plots of the volumetric strain at the free surface on the eight selected individual sources (Figure 7). In the evaluation of the outputs, the following cautionary actions were adopted: i) I only consider the observations located within two fault-lengths from each source, because earthquakes affect also the dynamic stress that becomes dominant in the intermediate and far field); ii) I only take into account observations placed inside the main deformation lobes and far from nodal lines, as a rectangular uniform-slipping source does not completely consider the faulting details; iii) I discount observations placed over a 1-km-wide zone across the fault trace(s) to avoid local slip heterogeneities that, near a fault, can originate strain changes that do not depend on the regional strain field. More detailed methodological aspects of this approach are fully described in Muir-Wood and King, (1993) and in Cucci, (2019).

I comprised in the calculations the observations up to two fault-lengths distance (up to 50–125 km, see Table 1) from each source, which is the reach where the most remarkable hydrological variations can be expected and where there is the highest chance to discriminate between models (Quilty and Roeloffs, 1997; Manga et al., 2003). To determine the investigated sources that better match the observed hydrological variations I only picked the sources with more than 50% of points of agreement between the polarities of the observed hydrological effects and the expected deformation (within the two fault-lengths distance). The findings of the elaboration are displayed in Table 3; only three sources out of eight (Valentini, Galli_Peronace, Jacques; all NW-verging) show satisfactory percentages (>50%) of agreement between expected and observed strain.


FIGURE 6
Examples of the coseimic environmental effecs reproduced by the architect Schiantarelli during the expedition headed by M. Sarconi. The left drawing faithfully illustrates a sand venting along the banks of river Mesima. The original writing below the image says "circular spots on the banks of Mesima". This observation corresponds to record n. 14 in Table 2. The central image "quasi circular depression of the ground near Polistena, and lake there produced" testifies of water emission and of the formation of a small lake. Two members of the expedition test the lake and measure its depth. This observation corresponds to record n. 39 in Table 2. The right etching ("lowering of the road to Casalnuovo") shows remarkable ground ruptures near Casalnuovo (presently Cittanova). Schiantarelli and another member of the expedition take measures of the displacement across the steps of the fractures. Galli and Bosi (2002) interpreted this site as evidence of surface faulting along the Cittanova Fault.

TABLE 2 List of the hydrological effects associated with the 1783 earthquake (progressive number corresponds to Fig. 5). The attribution of the quality code to the 78 effects is based on the reliability of the reference/account associated with the observation (see main text). The epicentral distance (in kilometers) is calculated from the location of the Italian seismic Catalogue (Rovida et al., 2021).

| NO. | Locality | Lat. | Lon. | Ep. Dist. | Evidence | Code | Notes | Reference |
|---|---|---|---|---|---|---|---|---|
| 1 | Acquaro | 38.555 | 16.19 | 34.4 | mixed water and sand venting | A | loc. Fontana | Blumetti et al. (2015); Sarconi (1784) |
| 2 | Anoia superiore | 38.429 | 16.115 | 19.3 | flow from spring disappeared | A | | De Leone (1783); Vivenzio (1783); Vivenzio (1788) |
| 3 | Bagnara Calabra | 38.287 | 15.805 | 14.3 | flow from public fountains disappeared | A | loc. Sperone and loc. Torre; uncertain association with 5th February mainshock | Botta (1832); De Leone (1783); Sarconi (1784) |
| 4 | Calanna | 38.184 | 15.723 | 25.1 | water emission, mixed water and sand venting, mud volcanoes | B | | De Leone (1783); Blumetti et al. (2015); Sarconi (1784) |
| 5 | Casalnuovo (Cittanova) | 38.374 | 16.086 | 13.2 | flow from River Vacale stopped | A | just North of the village | Caristina 1786; De Leone (1783); Grimaldi 1784; Vivenzio (1783); Vivenzio (1788) |
| 6 | Casalnuovo (Cittanova) | 38.345 | 16.079 | 10.9 | flow from Stream Serra stopped | A | South of the village | Caristina 1786; De Leone (1783); Vivenzio (1783); Vivenzio (1788) |
| 7 | Castellace | 38.323 | 15.953 | 3.2 | mixed water and sand venting, mud volcanoes | A | Fiumara Boscaino | De Dolomieu 1785; Blumetti et al. (2015) |
| 8 | Cinquefrondi | 38.406 | 16.1 | 16.6 | water emission, mixed water and sand venting, mud volcanoes | A | loc. Ventriconi | Blumetti et al. (2015); Galli (2000) |
| 9 | Cinquefrondi | 38.424 | 16.093 | 17.7 | emission of water | A | loc. Giardinetto | Grimaldi 1784; Vivenzio (1783); Vivenzio (1788) |
| 10 | Coccorino | 38.601 | 15.872 | 34.7 | mixed water and sand venting, mud volcanoes | A | | Blumetti et al. (2015); Galli (2000) |
| 11 | Cosoleto vecchio | 38.283 | 15.924 | 4.3 | water emission, mud volcanoes | A | | Blumetti et al. (2015); Galli (2000) |
| 12 | Dasà | 38.564 | 16.194 | 35.5 | mixed water and sand venting, mud volcanoes | A | | Blumetti et al. (2015); Sarconi (1784) |
| 13 | Dinami | 38.55 | 16.124 | 31.1 | sand venting, mud volcanoes; possibly affected by rainfall | B | loc. Ponte di Soreto over River Marepotamo | Sarconi (1784) |
| 14 | Fondaco di Borrello | 38.504 | 16.06 | 24.4 | emission of sulphurous water, mixed water and sand venting, mud volcanoes | A | 2 km NW of the village | De Leone (1783); Blumetti et al. (2015); Sarconi (1784); Vivenzio (1783); Vivenzio (1788) |
| 15 | Francica | 38.611 | 16.152 | 38.4 | sand venting, mud volcanoes; possibly affected by rainfall | B | 5 km East of the village along the River Mesima; uncertain location | Sarconi (1784) |
| 16 | Galatoni | 38.339 | 16.036 | 7.4 | emission of water | A | phenomenon lasted few hours | Grimaldi 1784 |
| 17 | Gallico marina | 38.163 | 15.651 | 31.7 | water emission, mixed water and sand venting, mud volcanoes | A | | De Leone (1783); Blumetti et al. (2015); Vivenzio (1783); Vivenzio (1788) |
| 18 | Gerocarne | 38.595 | 16.214 | 39.3 | mixed water and sand venting, mud volcanoes | A | along the road to Soriano | Botta (1832); Blumetti et al. (2015) |
| 19 | Gioia Tauro | 38.428 | 15.892 | 16 | water emission | A | | Carbone Grio (1884); Blumetti et al. (2015); Faggiotto (1895); Gallo (1784) |
| 20 | Iatrinoli | 38.354 | 16.008 | 7.1 | water emission | A | phenomenon lasted few hours | Grimaldi 1784 |
| 21 | Jaci (Acireale) | 37.605 | 15.168 | 104.2 | temporary decrease of the flow and chemical-physical variations of the local thermal springs | A | lasted short time | Gusta (1783) |
| 22 | Joppolo | 38.584 | 15.897 | 32.5 | mixed water and sand venting, mud volcanoes | A | | Blumetti et al. (2015); Galli (2000) |
| 23 | Laureana di Borrello | 38.492 | 16.067 | 23.3 | emission of turbid water; mixed water and sand venting (sand boils), mud volcanoes | A | c. Vaticano | Carbone Grio (1884); De Leone (1783); Hamilton (1784); Sarconi (1784); Vivenzio (1783); Vivenzio (1788) |
| 24 | Lubrichi | 38.27 | 15.955 | 3.3 | | A | west bank River Lago | |

(Continued on following page)

TABLE 2 (*Continued*) List of the hydrological effects associated with the 1783 earthquake (progressive number corresponds to Fig. 5). The attribution of the quality code to the 78 effects is based on the reliability of the reference/account associated with the observation (see main text). The epicentral distance (in kilometers) is calculated from the location of the Italian seismic Catalogue (Rovida et al., 2021).

| NO. | Locality | Lat. | Lon. | Ep. Dist. | Evidence | Code | Notes | Reference |
|---|---|---|---|---|---|---|---|---|
| | | | | | mixed water and sand venting, mud volcanoes | | | Botta (1832); Blumetti et al. (2015) |
| 25 | Maida marina | 38.862 | 16.229 | 66.6 | mixed water and sand venting | A | phenomenon lasted 1 day | Blumetti et al. (2015); Vivenzio (1783); Vivenzio (1788) |
| 26 | Maropati | 38.421 | 16.111 | 18.4 | mixed water and sand venting, mud volcanoes | A | loc. Eja | Blumetti et al. (2015); Galli (2000) |
| 27 | Maropati | 38.433 | 16.1 | 18.9 | water emission, mixed water and sand venting, mud volcanoes | A | loc. Scigalà | Blumetti et al. (2015); Sarconi (1784); Vivenzio (1783); Vivenzio (1788) |
| 28 | Messina | 38.188 | 15.553 | 38.5 | flow from public fountains disappeared | A | phenomenon lasted few days | Augusti (1783); Grimaldi 1784; Vivenzio (1783); Vivenzio (1788) |
| 29 | Messina | 38.188 | 15.553 | 38.5 | water emission, mud volcanoes | B | unverified description | Blumetti et al. (2015); Galli (2000) |
| 30 | Mileto vecchio | 38.595 | 16.078 | 34.4 | sand venting, mud volcanoes; possibly affected by rainfall | B | doubtful evidence of liquefaction | Grimaldi 1784 |
| 31 | Molochio | 38.309 | 16.033 | 5.7 | emission of brackish water | A | phenomenon lasted few hours | Caristina 1786; De Leone (1783); Grimaldi 1784; Vivenzio (1783); Vivenzio (1788) |
| 32 | Montauro | 38.749 | 16.511 | 68.9 | turbid flow from stream Fiumarella | B | reported before the occurrence of the event; generic description | Sarconi (1784) |
| 33 | Nicotera | 38.537 | 15.94 | 26.8 | emission of sulphureous hot water | A | loc. Ravello | Blumetti et al. (2015); Greco (1856); Sarconi (1784); Vivenzio (1783); Vivenzio (1788) |
| 34 | Oppido Mamertina | 38.285 | 15.999 | 2.9 | liquefaction | A | River Cumi | Botta (1832) |
| 35 | Oppido vecchia | 38.303 | 15.97 | 0.7 | flow from River Petrace disappeared | C | phenomenon lasted few hours; originated by damming caused by a landslide | Grimaldi 1784 |
| 36 | Oppido vecchia | 38.303 | 15.969 | 0.7 | water emission, mixed water and sand venting, mud volcanoes | A | loc. Nicolella | Blumetti et al. (2015); Sarconi (1784) |
| 37 | Oppido vecchia | 38.287 | 15.971 | 1.1 | water emission, mixed water and sand venting, mud volcanoes | A | River Tricuccio | Botta (1832); De Dolomieu 1785; Blumetti et al. (2015); Sarconi (1784) |
| 38 | Paracorio-Pedavoli (Delianuova) | 38.235 | 15.917 | 8.3 | mixed water and sand venting, mud volcanoes | A | | Botta (1832); Blumetti et al. (2015) |
| 39 | Polistena | 38.4 | 16.085 | 15.2 | mixed water and sand venting | A | C. Giuseppina | Carbone Grio (1884); De Dolomieu 1785; Blumetti et al. (2015); Sarconi (1784) |
| 40 | Polistena | 38.405 | 16.069 | 14.8 | increased flow from sulphurous cold spring | A | phenomenon lasted few days | De Dolomieu 1785 |
| 41 | Polistena | 38.399 | 16.065 | 14 | increased flow from River Vacale | A | | Grimaldi 1784 |
| 42 | Radicena (Taurianova) | 38.344 | 16.017 | 6.6 | emission of sulphurous hot water | A | banks of Torrente Razza | Caristina 1786; De Leone (1783); Greco, 1856; Grimaldi 1784; Vivenzio (1783); Vivenzio (1788) |
| 43 | Radicena (Taurianova) | 38.344 | 16.017 | 6.6 | Liquefaction | A | banks of Torrente Razza | Caristina 1786; De Leone (1783); Grimaldi 1784; Vivenzio (1783); Vivenzio (1788) |
| 44 | Radicena (Taurianova) | 38.352 | 16.005 | 6.8 | flow from fountain disappeared | A | temporary phenomenon | Caristina 1786; De Leone (1783); Grimaldi 1784; Vivenzio (1783); Vivenzio (1788) |
| 45 | Reggio Calabria | 38.116 | 15.649 | 34.6 | | A | loc. I Giunchi (via Giunchi) | |

(Continued on following page)

TABLE 2 (*Continued*) List of the hydrological effects associated with the 1783 earthquake (progressive number corresponds to Fig. 5). The attribution of the quality code to the 78 effects is based on the reliability of the reference/account associated with the observation (see main text). The epicentral distance (in kilometers) is calculated from the location of the Italian seismic Catalogue (Rovida et al., 2021).

| NO. | Locality | Lat. | Lon. | Ep. Dist. | Evidence | Code | Notes | Reference |
|---|---|---|---|---|---|---|---|---|
| | | | | | water emission, mixed water and sand venting, mud volcanoes | | | De Leone (1783); Galli (2000); Vivenzio (1783); Vivenzio (1788) |
| 46 | Rosarno | 38.501 | 15.987 | 22.7 | increased discharge and turbid flow of River Mesima | A | | De Leone (1783); Grimaldi 1784; Vivenzio (1783); Vivenzio (1788) |
| 47 | Rosarno | 38.501 | 15.987 | 22.7 | stream flow stopped | B | temporary phenomenon; doubtful evidence | Hamilton (1784) |
| 48 | Rosarno | 38.498 | 15.978 | 22.3 | liquefaction on the banks of River Mesima | A | | Augusti (1783); Carbone Grio (1884); De Leone (1783); Vivenzio (1783); Vivenzio (1788) |
| 49 | Rosarno | 38.528 | 16.002 | 25.8 | multiple liquefactions | A | ford on Torrente Mammella (loc. ponte Mammella) | Hamilton (1784) |
| 50 | Rosarno | 38.528 | 16.002 | 25.8 | stream flow stopped | B | temporary phenomenon (loc. ponte Mammella); doubtful evidence | Hamilton (1784) |
| 51 | S. Cristina d'Aspromonte | 38.253 | 15.96 | 5 | mud and sand venting | A | | Blumetti et al. (2015); Galli (2000) |
| 52 | S. Martino | 38.36 | 15.978 | 7 | emission of water | A | phenomenon lasted few hours | Grimaldi 1784 |
| 53 | San Fili (Melicucco) | 38.455 | 16.03 | 18.3 | water emission, mixed water and sand venting, mud volcanoes | A | along the banks of River Vacale | Blumetti et al. (2015); Sarconi (1784) |
| 54 | San Lucido | 39.305 | 16.058 | 112.1 | sand venting, mud volcanoes | B | former lake of Monte S. Giovanni | Blumetti et al. (2015); Galli (2000); Sarconi (1784) |
| 55 | San Procopio | 38.281 | 15.901 | 6.3 | flow from Fiumara Sevina almost disappeared | A | phenomenon lasted 2 days | Galimi (1783) |
| 56 | San Procopio | 38.282 | 15.89 | 7.2 | mixed water and sand venting, mud volcanoes | B | loc. Fabrizia; uncertain location | Galimi (1783) |
| 57 | San Procopio | 38.287 | 15.899 | 6.3 | formation of new spring | A | c Rasalà | Galimi (1783) |
| 58 | San Procopio | 38.292 | 15.902 | 6 | mud volcanoes | C | loc. La Goletta; uncertain location | Blumetti et al. (2015); Galimi (1783) |
| 59 | San Procopio | 38.283 | 15.884 | 7.7 | sand venting, mud volcanoes | A | C. Ruffino | Blumetti et al. (2015); Galimi (1783) |
| 60 | San Procopio | 38.279 | 15.881 | 8 | mud volcanoes | A | loc. Bombardara along the road to Sinopoli | Blumetti et al. (2015); Galimi (1783) |
| 61 | Sant'Anna di Seminara | 38.322 | 15.89 | 7.5 | emission of water | A | loc. Scaddarito | Carbone Grio (1884); Blumetti et al. (2015); Galli (2000); Gallo (1784) |
| 62 | Satriano | 38.674 | 16.49 | 61.6 | turbid flow from stream Ancinale | B | reported before the occurrence of the event; generic description | Sarconi (1784) |
| 63 | Scido | 38.244 | 15.938 | 6.5 | sand venting | A | | Botta (1832); Blumetti et al. (2015) |
| 64 | Scido | 38.255 | 15.938 | 5.4 | sand venting, mud volcanoes | A | loc. Santa Giorgia | Botta (1832); Blumetti et al. (2015) |
| 65 | Scroforio | 38.332 | 16.018 | 5.7 | water emission, mixed water and sand venting, mud volcanoes | C | loc. Fiumara secca; not associated with 5th February mainshock | Blumetti et al., 2015 |
| 66 | Scroforio | 38.339 | 16.009 | 5.8 | sand venting, mud volcanoes | A | | Sarconi (1784) |
| 67 | Scroforio | 38.335 | 16.018 | 5.9 | mixed water and sand venting, mud volcanoes | A | | Blumetti et al. (2015); Grimaldi 1784 |
| 68 | Seminara | 38.334 | 15.874 | 9.3 | water emission, mud volcanoes | A | | Blumetti et al. (2015); Galli (2000) |
| 69 | Seminara | 38.339 | 15.873 | 9.7 | Liquefaction | A | loc. L'Annunziata | De Leone (1783); Vivenzio (1783); Vivenzio (1788) |
| 70 | Seminara | 38.375 | 15.88 | 11.7 | emission of hot water | A | loc. Pietre Negre | Gallo (1784) |
| 71 | Sitizano | 38.282 | 15.94 | 3.1 | sand venting, mud volcanoes | B | doubtful evidence of liquefaction | Blumetti et al. (2015); Gallo (1784) |

(Continued on following page)

TABLE 2 (*Continued*) List of the hydrological effects associated with the 1783 earthquake (progressive number corresponds to Fig. 5). The attribution of the quality code to the 78 effects is based on the reliability of the reference/account associated with the observation (see main text). The epicentral distance (in kilometers) is calculated from the location of the Italian seismic Catalogue (Rovida et al., 2021).

| NO. | Locality | Lat. | Lon. | Ep. Dist. | Evidence | Code | Notes | Reference |
|---|---|---|---|---|---|---|---|---|
| 72 | Terranova Sappo Minulio | 38.311 | 16.006 | 3.5 | flow from fountain disappeared | A | 1 km S of the village | Sarconi (1784) |
| 73 | Terranova Sappo Minulio | 38.311 | 16.006 | 3.5 | sand venting, mud volcanoes | A | 1 km S of the village | Sarconi (1784) |
| 74 | Terranova Sappo Minulio | 38.321 | 16.009 | 4.3 | water emission, mixed water and sand venting | A | courtyard of the Celestini Friars Monastery | Blumetti et al. (2015); Galli (2000); Lyell (1868) |
| 75 | Torre Faro | 38.265 | 15.643 | 28.8 | sand venting, mud volcanoes | A | | De Leone (1783); Blumetti et al. (2015) |
| 76 | Tresilico | 38.303 | 15.979 | 1 | water emission | A | | Blumetti et al. (2015); Galli (2000) |
| 77 | Tropea | 38.664 | 15.895 | 41.2 | mixed water and sand venting, mud volcanoes | A | | Despuig (1895) |
| 78 | Varapodio | 38.311 | 15.988 | 2.2 | water emission, mixed water and sand venting, mud volcanoes | A | | Blumetti et al. (2015); Galli (2000) |

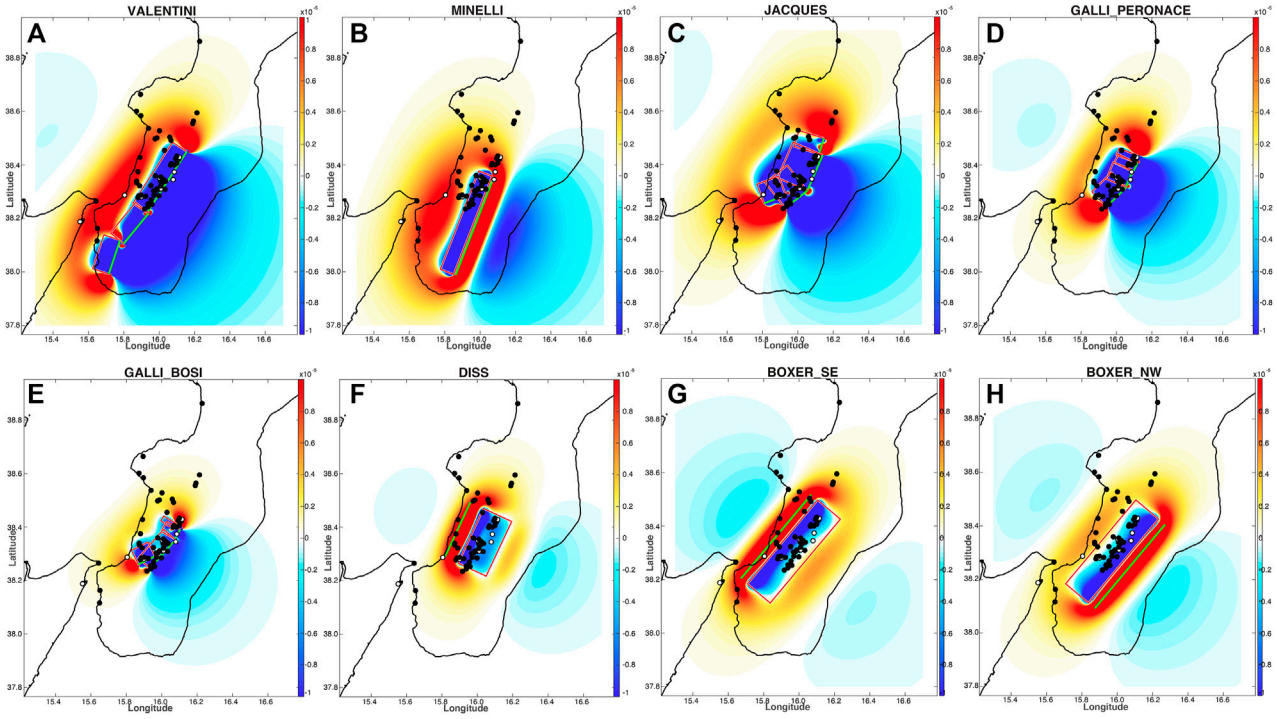


FIGURE 7
Comparison between the calculated coseismic strain fields along eight potential sources and the observed hydrological effects produces by the 1783 earthquake. In the plots of strain, blue shading indicates areas in compression, and red shading areas in dilatation. The input parameters of the Coulomb 3.4 code are: Poission's ratio 0.25; Young's modulus 8 x $10^5$ bars; friction coefficient 0.4; shear modulus 3.3 x $10^5$ bars. For the output the dilatational strain is assumed positive. Units: $10^{-5}$. A red rectangle indicates the surface projection of the fault plane; a green line is the intersection of the updip projection of the fault with the surface. Streamflow changes are indicated by circles (black/discharge increase; white/discharge decrease). An increase in discharge is expected in compressional areas, and a streamflow decrease in dilatational areas.

# 7 Discussion

A couple of general considerations can be put forward about the quality and the consistency of the hydrological dataset investigated, along with the distribution of the data. The 63 hydrological observations that were utilized to discriminate between models constitute by far the most considerable dataset when it is compared to the number of data employed in this type of analyses (see papers cited above), also considering that the observations refer to a 250 years-old earthquake. This evidence also confirms the extraordinary work carried out by the coeval reporters in the field. Also, the distance between the data points and each investigated source is a critical issue; the average distance between all the 504 data points located within two fault-lengths and each source is 18.2 km, a value that supports the need to observe the coseismic hydrological changes in the near-field of a seismogenic source. Finally, an analysis of Table 2 that summarizes the hydrological observations confirms that the majority of the data (54 out of 63) consists of positive emission of water associated with compressional strain changes (increase of discharge of river and spring flows, the raised level in wells, liquefaction). This behavior is frequently observed around normal fault earthquakes (Muir-Wood and King, 1993) and is a strong indication of the most likely style of faulting affecting this region.

When considering the performance of the candidate sources in relation to their geometry and sense of dip, the first piece of evidence is that both the SE-dipping faults (DISS, Boxer_SE; Figure 4, Figures 7F,G) show a poor fit between expected deformation pattern and distribution of the hydrological observations. A possible explanation of this behavior is that these potential sources share a common feature in their minimum depth (2–3 km), i.e., they are blind faults that originate more subdued coseismic fields of strain that can hardly affect many hydrological points. In addition, the magnitude associated with the DISS source (Mw6.6, from empirical relationships) and the consequent field of deformation seem underestimated when compared to the other potential sources and to the magnitude reported in the Catalogue.

Among the NW-dipping faults, the general pattern of strain originated by the candidate sources Minelli, Galli_Bosi and Boxer_NW (Figures 3, Figures 7B,E,H) does not provide an acceptable fit with the observed hydrological changes. In particular, the location of the source Minelli, based on magnetic data and modeling (Figure 7B), appears significantly shifted southward with respect to the distribution of the most important effects of the 1783 earthquake (intensities, hydrological changes, coseismic ruptures), whilst the strain field produced by the source Galli_Bosi (Figure 7E) is of limited extent due to its magnitude (Mw6.5, see Table 1), significantly lower than that of the seismic Catalogue (Rovida et al., 2021). Finally, both the earthquake sources (Boxer_NW and Boxer_SE, Figures 7G,H) that were derived from inversion of intensity data display unsatisfactory results, as in this case the barycenter of the region of the largest earthquake effects does not fully coincide with the area of distribution and with the polarities of the hydrological signatures.

Let us consider now the three potential seismogenic sources that display the best fit (Figures 7A,C,D). They share several distinctive features besides the same vergence direction, as they all consist of systems of three to four surface-rupturing fault segments capable of generating individual earthquakes with comparable magnitude in the interval M6.9-M7.1. However, I observe that the contribution to the total strain field of the two southernmost segments of the Valentini source (Figure 7A) does not substantially improve the fit between observed data and expected deformation, thus these two segments, far off the epicenter and the area of maximum damage, can be considered as secondary faults from the perspective of the hydrological response. Conversely, the geometry and the location of the Galli_Peronace and of the Jacques sources (that display the best percentage 0.56 and 0.66, respectively) are quite similar (Figures 7C,D), as they insist over the area of maximum effects and almost coincide with the 20 km-long coseismic surface fracturing described by De Dolomieu and by many other reporters soon after the event. However, the performance of the Jacques source (Figure 7C, Figure 8) is higher than that of Galli_Peronace, and lines up with the best results shown for the investigation on other historical events in similar studies (see papers cited above).

A possible twofold explanation to this issue is proposed as follows: i) the Jacques source envisions a much thicker seismogenic layer than all the other investigated sources (see Table 1), and ii) Jacques et al. (2001) include two additional fault strands, located North (Galatro Fault) and South (S. Eufemia Fault) of the Cittanova Fault, in the 1783 earthquake source (Figure 8). Both the above-described features are specific to the Jacques source and allow to better define the width and the depth of the seismogenic volume involved in the variation of crustal porosity. Besides the individuation of the Cittanova Fault system as the most probable seismogenic source of the 5 February 1783 earthquake, the present research can put forward general observations and clues concerning the kinematics, the seismotectonics, and the hydrogeological signature of the study area. There is a clear indication from the plots of strain that deformation along NW-verging, ~45 km-long, ~20 km-wide surface-rupturing systems of normal faults provides the best fit with the hydrological response following a 1783-type earthquake (Figure 7A,C and D). This is a common style of faulting in the region, since it has been testified by paleoseismological studies and direct observations for some of the most energetic historical and modern earthquakes that occurred in Central (Galli and Bosi 2002), and Northern Calabria (Cinti et al., 1997; 2002), as well as in the Southern Apennines (Pantosti et al., 1993), though there are some exceptions (see for instance the oblique blind fault

TABLE 3 Comparison between the deformation expected on the eight potential sources and the polarities of the 63 rank 'A' coseismic observations. The upper row shows the ratio between the number of polarities consistent with the expected deformation and the total number of observations. The lower row indicates the corresponding values in percentage. Values of percentage >50% are shown in bold and are associated with the three best fit seismogenic sources.

| Valentini | Minelli | Jacques | Galli_Peronace | Galli_Bosi | DISS | Boxer_SE | Boxer_NW |
|---|---|---|---|---|---|---|---|
| 35/63 | 27/63 | 41/62 | 35/62 | 29/61 | 30/62 | 31/63 | 31/63 |
| **56** | 43 | **66** | **56** | 47 | 48 | 49 | 49 |

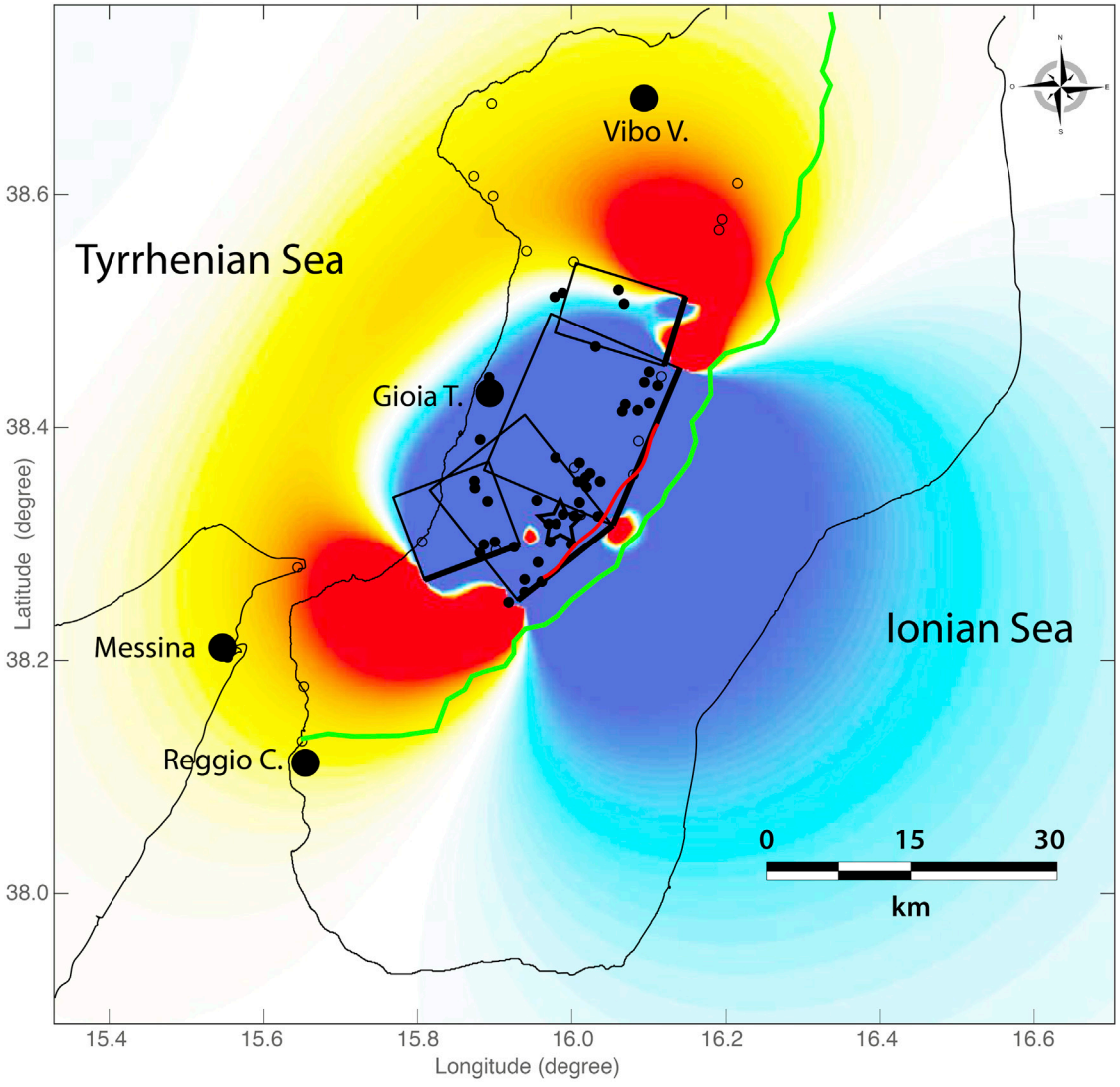


FIGURE 8
Coseismis strain field induced by the Jacques potention source of the 1783 earthquake. Blue shading indicates areas in compression red shading areas in dilatation. Units:$10^{-5}$. The thicker black line is the intersection of the updip projection of each fault segment with the surface. Circles show the location of all the observed hydrological effects (both positive and negative) that are in agreement (solid circles) or in disagreement (empty circles) with the expected deformation. A red line marks the pattern of the 20 km-long surface ruptures observed in the ground after the event. A green line shows the location of the watershed of the drainage between the Tyrrhenian Sea (West) and the Ionian Sea (East).

responsible for the M6.7 seismic event that occurred in Irpinia in 1930, Cucci 2019). An indication that stems from the calculations of strain and which is closely tied to the geometry and seismic behaviour of the 1783 earthquake source regards the minimum magnitude of the seismic event, that I propose to set at M≥7.0 (comparable to that inferred by macroseismic data and reported in the Catalogue), based on the pattern of hydrological response; sources characterized by magnitudes lower than that threshold would not be capable of generating the hydrological signature that was observed in the field.

Finally, the results of this study cast light on the significance of the fracturing reported by De Dolomieu in the aftermath of the shock; even though this coseismic feature mostly coincides with the Cittanova Fault and in particular with the location of the Jacques source (Figure 8), it was questioned by some investigators as the intersection of the actual earthquake fault with the free surface. However, the pattern of the hydrological response supports the hypothesis that the 20 km-long surface ruptures reflect primary faulting. An interesting observation that is possibly linked to this evidence is the absence of hydrological changes of any type along the Ionian (Eastern) side of the epicentral area (Figure 8), though the presence of the rugged Aspromonte Massif can possibly affect this pattern. Although there are remarkable differences in the geological and geomorphological setting between the Tyrrhenian and the Ionian sides, I want to emphasize the possibility that the Cittanova Fault and the adjacent system of faults may play a role in the overall hydrogeological circulation of this area. As the whole hydrological circuit depends on rock permeability, and permeability changes can occur as a consequence of faulting activity, there is the possibility that the Cittanova system of faults acts as a hydrological barrier that hampers the groundwater circulation toward the East (Italiano et al., 2010; Cianflone et al., 2021).

## 8 Conclusion

I studied the coseismic hydrological variations induced by the M7.1 (Rovida et al., 2021) 1783 Southern Calabria earthquake to verify if they can be explained by the coseismic static strain and pore pressure change predicted by the poroelastic theory (Wakita 1975). To this aim, I compared the strain field induced by eight potential seismogenic sources with the distribution of the groundwater anomalies reported after the earthquake, searching for correspondence between the observed hydrological variations (increase/decrease of water flow) and the expected strain signatures (compression/dilatation). The hydrological dataset consisted of 78 observations of hydrological changes that occurred following the 1783 seismic event in 53 different localities.

The most important outcomes of the present study can be summarized as follows: a) the group of potential sources that display the best agreement between expected strain and hydrological signature consists of NW-verging systems of three to four surface-rupturing almost pure normal fault segments capable of originating earthquakes with magnitude in the interval Mw6.9-M7.1; among these, my study favors the source proposed by Jacques et al (2001), which envisions a 18 km-thick seismogenic layer and additional fault strands besides the Cittanova Fault; b) the distribution of the observed coseismic hydrological anomalies does not support the role of the SE-dipping faults (DISS, Boxer_SE) as potential sources of the 1783 earthquake, mainly because the deformation imposed by those blind faults, in addition to the relatively low magnitude (DISS) or to the low angle of dip (Boxer_SE), hardly affects many hydrological points; c) the pattern of deformation associated with the Jacques source and the location of the Cittanova Fault support the hypothesis that the 20 km-long surface ruptures testified soon after the 1783 event reflect primary faulting; d) a minimum magnitude M6.9–7.0 is required to obtain the pattern and the extent of distribution of the coseismic hydrological changes observed in the field after the 1783 event; e) the location of the hydrological variations that were observed only along the Tyrrhenian (western) side of southern Calabria can be evidence that the Cittanova system of faults might be a hydrological barrier that hampers the groundwater circulation toward the East.

I want to emphasize some final considerations regarding the implications of this kind of studies. Previous papers dealing with the same methodologies employed in the present work yielded important contributions to discriminate among the seismogenic sources proposed for some large magnitude earthquakes that occurred in the past two centuries in adjacent areas of Calabria and Southern Apennines (Tertulliani and Cucci, 2009; Cucci, 2019). Provided that the available dataset of hydrological observations must be quantitatively consistent and accurately verified–as in the case of the 1783 Calabria event shown in this paper–the hydrological signature of an earthquake can provide tools to widen our knowledge of historical earthquakes and decisive constraints on their causative faults.

## Data availability statement

The datasets presented in this study can be found in online repositories. The names of the repository/repositories and accession number(s) can be found in the article/supplementary material.
The 1783 coseismic hydrological changes are available at: https://figshare.com/articles/dataset/1783_coseismic_hydrological changes_docx/20036522.
BOXER 4.1 code is available at https://emidius.mi.ingv.it/boxer/.
DISS, Database of Individual Seismogenic Sources (DISS), is available at: https://doi.org/10.13127/diss3.3.0.
ITHACA, Database of active capable faults of the Italian territory, is available at: http://sgi.isprambiente.it/ithaca/viewer/index.html.

CPTI, Catalogo Parametrico dei Terremoti Italiani, is available at: https://doi.org/10.13127/CPTI/CPTI15.3.
CFTI, Catalogue of strong earthquakes in Italy and in the Mediterranean area, is available at: https://doi.org/10.1038/s41597-019-0091-9.
The topographic maps at 1:10.000 scale are available at https://geoportale.regione.calabria.it. The topographic maps at 1:25.000 scale are available at: https://www.igmi.org/.

## Author contributions

LC conceived, elaborated and wrote the manuscript.

## Acknowledgments

I want to thank the Editor N.A. Pino and three reviewers for their comments and suggestions. Thanks to L. Graziani for her support in the run of the code Boxer, and to G. Vannucci for useful information about that software. Thanks to A. Tertulliani for his valuable help in the traffic of ancient documents of the historical archive of our Institute, and to L. Alfonsi who provided important suggestions on a previous version of the manuscript.

## Conflict of interest

The authors declare that the research was conducted in the absence of any commercial or financial relationships that could be construed as a potential conflict of interest.

## Publisher's note



## References

Augusti, M. (1783). *Dei terremoti di Messina, e di Calabria dell'anno 1783, memorie e riflessioni*. Bologna.

Blumetti, A.M., Guerrieri, L., and Porfido, S. (2015). "Cataloguing the EEEs induced by the 1783 5th February Calabrian earthquake: implications for an improved seismic hazard," in *Earthquake Environmental Effect for seismic hazard assessment: the ESI intensity scale and the EEE Catalogue, Memorie descrittive della carta geologica d'Italia*. Editor L. Guerrieri, 153–164.

Botta, V.C. (1832). *Storia d'Italia continuata da quella del Guicciardini sino al 1789*. Paris: Baudry.

Carbone-Grio, D. (1884). *I terremoti di Calabria e di Sicilia nel secolo XVIII*. De 520 Angelis e Figlio, Napoli.

Caristina, D. (1786). *Diatriba historico-physica de terraemotu calabro*. Napoli.

Chiarabba, C., De Gori, P., and Speranza, F. (2008). The southern Tyrrhenian subduction zone: Deep geometry, magmatism and Plio-Pleistocene evolution. *Earth Planet. Sci. Lett.* 268, 408–423. doi:10.1016/j.epsl.2008.01.036

Cianflone, G., Vespasiano, G., De Rosa, R., Dominici, R., Apollaro, C., Vaselli, O., Pizzino, L., Tolomei, C., Capecchiacci, F., and Polemio, M. (2021). Hydrostratigraphic Framework and Physicochemical Status of Groundwater in the Gioia Tauro Coastal Plain (Calabria-Southern Italy). *Water* 13, 3279. doi:10.3390/w13223279

Cinti, F. R., Cucci, L., Pantosti, D., D'Addezio, G., and Meghraoui, M. (1997). A major seismogenic fault in a 'silent area': the Castrovillari fault (southern Apennines, Italy). *Geophys. J. Int.* 130, 595–605. doi:10.1111/j.1365-246x.1997.tb01855.x

Cinti, F. R., Moro, M., Pantosti, D., Cucci, L., and D'Addezio, G. (2002). New constraints on the seismic history of the Castrovillari fault in the Pollino gap (Calabria, southern Italy). *J. Seismol.* 6, 199–217. doi:10.1023/a:1015693127008

Coccia, G. (1783). Relazione al Maresciallo D. Francesco Pignatelli Vicario Generale di Calabria, per la distrutta città di S. Cristina, col tremoto del 5 febbraio 1783, Dall'Archivio Vescovile di Oppido. *Riv. Stor. Calabrese, S. Lucido, anno II* 10, 227–234.

Cotecchia, V., Guerricchio, A., and Melidoro, G. (1986). *International Symposium on Engineering Geology Problems in Seismic Areas*. Bari, Italy: Int. Assoc. of Eng. Geol.The geomorphogenetic crisis triggered by the 1783 earthquake in Calabria (southern Italy)

Cox, S.C., Rutter, H.K., Sims, A., Manga, M., Weir, J.J., Ezzy, T., White, P.A., Horton, T.W., and Scott, D. (2012). Hydrological effects of the MW 7.1 Darfield (Canterbury) earthquake, 4 September 2010, New Zealand. *New Zealand Journal of Geology and Geophysics* 55 (3), 231–247. doi:10.1080/00288306.2012.680474

Cucci, L. (2019). Insights into the geometry and faulting style of the causative faults of the M6.7 1805 and M6.7 1930 earthquakes in the Southern Apennines (Italy) from coseismic hydrological changes. *Tectonophysics* 751, 192–211. doi:10.1016/j.tecto.2018.12.021

Cucci, L., and Tertulliani, A. (2015). The hydrological signature of a seismogenic source: coseismic hydrological changes in response to the 1915 Fucino (Central Italy) earthquake. *Geophys. J. Int.* 200, 1374–1388. doi:10.1093/gji/ggu448

De Dolomieu, D. (1784). *Memoria Sopra i Tremuoti della Calabria nell'Anno 1783*. Salvioni, Roma.

De Leone, A. (1783). *Giornale e notizie de' tremuoti accaduti l'anno 1783 nella provincia di Catanzaro*. Parte Prima, Raimondi, Napoli.

Despuig, A. (1895). "Il terremoto calabrese del 1783," in *Le osservazioni di Antonio Despuig sul terremoto calabrese del 1783. Incontri Meridionali. Rivista di storia e cultura*. Editor C. Carlino, 69–79.

DISS Working Group (2021). *Database of Individual Seismogenic Sources (DISS), Version 3.3.0: A compilation of potential sources for earthquakes larger than M 5.5 in Italy and surrounding areas*. Istituto Nazionale di Geofisica e Vulcanologia. doi:10.13127/diss3.3.0

Faccenna, C., Becker, T. W., Lucente, F. P., Jolivet, L., and Rossetti, F. (2001). History of subduction and back-arc extension in the Central Mediterranean. *Geophys. J. Int.* 145, 809–820. doi:10.1046/j.0956-540x.2001.01435.x

Faccenna, C., Becker, T.W., Miller, M.S., Serpelloni, E., and Willett, S.D. (2014). Isostasy, dynamic topography, and the elevation of the Apennines of Italy. *Earth and Planetary Science Letters* 407, 163–174. doi:10.1016/j.epsl.2014.09.027

Faggiotto, A. (1895). *I terremoti calabro-siculi e loro probabili cause*. Reggio Calabria.

Galadini, F. (2022). Ruins and Remains as a Background: Natural Catastrophes, Abandonment of Medieval Villages, and the Perspective of Civilization during the 20th Century in the Central Apennines (Abruzzi Region, Central Italy). *Sustainability* 14, 9517. doi:10.3390/su14159517

Galimi, P. (1783). *Lettera di Procopio Galimi al signor D. Giuseppe Vairo su' tremuoti di Calabria dell'anno 1783*. Napoli.

Galli, P. (2000). New empirical relationships between magnitude and distance for liquefaction for liquefaction. *Tectonophysics* 324, 169–187. doi:10.1016/s0040-1951(00)00118-9

Galli, P., and Bosi, V. (2002). Paleoseismology along the Cittanova fault: Implications for seismotectonics and earthquake recurrence in Calabria (southern Italy). *J. Geophys. Res.* 107, 2044. doi:10.1029/2001JB000234

Galli, P. A. C., and Peronace, E. (2015). Low slip rates and multimillennial return times for Mw 7 earthquake faults in southern Calabria (Italy), *Geophys. Res. Lett*., 42, 5258–5265, doi:10.1002/2015GL064062

Galli, P., Scionti, V., and Spina, V. (2007). New paleoseismic data from the Lakes and Serre faults (Calabria, southern Italy). Seismotectonic implication. *Boll. Soc. Geol. It.* 126, 347–364.

Gallo, A. (1784). "Lettere scritte da Andrea Gallo pelli terremoti del 1783. Con un giornale meteorologico de' medesimi. Aggiuntavi anche la Relazione di quei di Calabria con li paesi distrutti, ed il numero de' morti. Di Stefano, Messina.

Gasperini, P., Vannucci, G., Tripone, D., and Boschi, E. (2010). The location and sizing of historical earthquakes using the attenuation of macroseismic intensity with distance. *Bull. Seismol. Soc. Am.* 100, 2035–2066. doi:10.1785/0120090330

Grecksch, G., Roth, F., and Kumpel, H.J. (1999). Coseismic well-level changes due to the 1992 Roermond earthquake compared to static deformation of half-space solutions. *Geophys. J. Int.* 138, 470–478. doi:10.1046/j.1365-246x.1999.00894.x

Greco, L.M. (1856). *Delle principali opere intorno ai calabri tremuoti dal 1783 al 1854 e degli studi più convenevoli sopra i medesimi*. Napoli.

Grimaldi, F.A. (1784). *Descrizione de' tremuoti accaduti nelle Calabrie nel 1783*. Porcelli, Napoli.

Guidoboni, E., Ferrari, G., Tarabusi, G., Sgattoni, G., Comastri, A., Mariotti, D., Ciuccarelli, C., Bianchi, M.G., and Valensise, G. (2019). CFTI5Med, the new release of the catalogue of strong earthquakes in Italy and in the Mediterranean area. *Sci. Data* 6, 80. doi:10.1038/s41597-019-0091-9

Gusta, F. (1783). *Stato felice ed infelice della Calabria e di Messina e del suo territorio prima e doppo i terremoti de' 5 febbrajo, e 28 marzo 1783, accaduti in quelle parti*. Pagani, Firenze, 1783.

Hamilton, M.W. (1784). *Relation des derniers tremblemens de terre arrivés en Calabre et en Sicile*. Barde, Geneve.

Hanks, T.C., and Kanamori, H. (1979). A moment magnitude scale. *J. Geophys. Res.* 84, 2348–2350. doi:10.1029/jb084ib05p02348

Italiano, F., Bonfanti, P., Pizzino, L., and Quattrocchi, F. (2010). Geochemistry of fluids discharged over the seismic area of the Southern Apennines (Calabria region, Southern Italy): Implications for Fluid-Fault relationships. *Applied Geochemistry* 25, 540–554. doi:10.1016/j.apgeochem.2010.01.011

ITHACA Working Group (2019). "ITHACA (ITaly HAzard from CApable faulting)," in *A database of active capable faults of the Italian territory* (ISPRA Geological Survey of Italy).

Jacques, E., Monaco, C., Tapponnier, P., Tortorici, L., and Winter, T. (2001). Faulting and earthquake triggering during the 1783 Calabria seismic sequence. *Geophys. J. Int.* 147, 499–516. doi:10.1046/j.0956-540x.2001.01518.x

Janku, A., Schenk, G.J., and Mauelshagen, F. (2012). *Historical disasters in context. Science, religion, and politics*. London: Taylor & Francis.

Locati, M., Camassi, R., Rovida, A., Ercolani, E., Bernardini, F., Castelli, V., Caracciolo, C.H., Tertulliani, A., Rossi, A., Azzaro, R., D'Amico, S., and Antonucci, A. (2022). *Database Macrosismico Italiano (DBMI15), versione 4.0*. Istituto Nazionale di Geofisica e Vulcanologia. doi:10.13127/DBMI/DBMI15.4

Lyell, C. (1868). *Principles of geology*. John Murray, Albermarle Street, London.

Malinverno, A., and Ryan, W. B. F. (1986). Extension in the Tyrrhenian Sea and shortening in the Apennines as result of arc migration driven by sinking of the lithosphere. *Tectonics* 5, 227–245. doi:10.1029/tc005i002p00227

Manga, M., Brodsky, E.E., and Boone, M. (2003). Response of streamflow to multiple earthquakes. *Geophys. Res. Lett.* 30, 1214. doi:10.1029/2002GL016618

Minelli, L., Vecchio, A., Speranza, F., Nicolosi, I., D'Ajello Caracciolo, F., Chiappini, S., Carluccio, R., and Chiappini, M. (2016). Aeromagnetic investigation of southern Calabria and the Messina Straits (Italy): Tracking seismogenic sources of 1783 and 1908 earthquakes. *J. Geophys. Res. Solid Earth* 121, 1297–1315. doi:10.1002/2015JB012305

Montgomery, D.R., and Manga, M. (2003). Streamflow and water well responses to earthquakes. *Science* 300, 2047–2049. doi:10.1126/science.1082980

Montgomery, D.R., Greenberg, H.M., and Smith, D.T. (2003). Streamflow response to the Nisqually earthquake. *Earth Planet. Sci. Lett.* 209, 19–28. doi:10.1016/s0012-821x(03)00074-8

Muir-Wood, R., and King, G.P. (1993). Hydrological signatures of earthquake strain. *J. Geophys. Res.* 98, 22035–22068. doi:10.1029/93jb02219

Okada, Y. (1985). Surface deformation due to shear and tensile faults in a half-space. *Bull. Seismol. Soc. Am.* 75 (4), 1135–1154. doi:10.1785/bssa0750041135

Pantosti, D., Schwartz, D.P., and Valensise, G. (1993). Paleoseismology along the 1980 surface rupture of the Irpinia Fault – Implications for earthquake recurrence in the Southern Apennines, Italy. *J. Geophys. Res.* 98, 6561–6577. doi:10.1029/92jb02277

Petitta, M., Mastrorillo, L., Preziosi, E., Banzato, F., Barberio, M. D., Billi, A., et al. (2018). Water-table and discharge changes associated with the 2016–2017 seismic sequence in central Italy: hydrogeological data and a conceptual model for fractured carbonate aquifers. *Hydrogeol. J.* 26 (4), 1009–1026. doi:10.1007/s10040-017-1717-7

Pizzino, L. P, Burrato, , F, Valensise, G., and Quattrocchi, F. (2004). Geochemical signatures of large active faults: The example of the 5 February 1783, Calabrian earthquake (southern Italy). *Journal of Seismology* 8, 363–380. doi:10.1023/b:jose.0000038455.56343.e7

Quilty, E.G., and Roeloffs, E.A. (1997). Water-level changes in response to the 20 December 1994 earthquake near Parkfield, California. *Bull. Seismol. Soc. Am.* 87, 310–317. doi:10.1785/bssa0870020310

Ricchetti, E., and Ricchetti, G. (1991). Aspetti della morfogenesi pleistocenico olocenica sul versante tirrenico della Calabria. *Mem. Soc. Geol. Ital.* 47, 655–663.

Rovida, A., Locati, M., Camassi, R., Lolli, B., Gasperini, P., and Antonucci, A. (2021). *Catalogo Parametrico dei Terremoti Italiani (CPTI15), versione 3.0*. Istituto Nazionale di Geofisica e Vulcanologia. doi:10.13127/CPTI/CPTI15.3

Sarconi, M. (1784). *Istoria de' fenomeni del tremoto avvenuto nelle Calabrie, e nel Valdemone nell'anno 1783 posta in luce dalla Reale Accademia delle Scienze, e delle Belle Lettere di Napoli*. Campo, Napoli.

Stucchi, M., Albini, P., Mirto, C., and Rebez, A. (2004). Assessing the completeness of Italian historical earthquake data. *Ann. Geophys.* 47, 659–673.

Tertulliani, A., and Cucci, L. (2009). Clues to the identification of a seismogenic source from environmental effects: the case of the 1905 Calabria (Southern Italy) earthquake. *Nat. Hazards Earth Syst. Sci.* 9, 1787–1803. doi:10.5194/nhess-9-1787-2009

Tiberti, M. M., Vannoli, P., Fracassi, U., Burrato, P., Kastelic, V., and Valensise, G. (2017). Understanding seismogenic processes in the southern Calabrian Arc: a geodynamic perspective. *Ital. J. Geosci.* 136, 365–388. doi:10.3301/IJG.2016.12

Toda, S., Stein, R.S., Sevilgen, V., and Lin, J. (2011). *Coulomb 3.3 Graphic-rich deformation and stress-change software for earthquake, tectonic, and volcano research and teaching - user guide: Rep. Earthquake Science Center*. Menlo Park, California: Menlo Park Science Center, 63.

Tortorici, L., Monaco, C., Tansi, C., and Cocina, O. (1995). Recent and active tectonics in the Calabrian arc (southern Italy). *Tectonophysics* 243, 37–55. doi:10.1016/0040-1951(94)00190-k

Valensise, G., and D'Addezio, G. (1994). *Il contributo della geologia di superficie all'identificazione delle strutture sismogenetiche della Piana di Gioia Tauro, Internal Rep*. Bologna, Italy: Ist. Naz. di Geofis., 21.

Valentini, A., Visini, F., and Pace, B. (2017). Integrating faults and past earthquakes into a probabilistic seismic hazard model for peninsular Italy. *Nat. Hazards Earth Syst. Sci.* 17, 2017–2039. doi:10.5194/nhess-17-2017-2017

Vivenzio, G. (1783). *Istoria e teoria de' tremuoti in generale ed in particolare di quelli della Calabria, e di Messina del 1783*. Napoli: Stamperia Regale, 462pp.

Vivenzio, G. (1788). *Istoria de' tremuoti avvenuti nella Provincia della Calabria Ulteriore, e nella città di Messina nell'anno 1783. E di quanto nella Calabria fu fatto per lo suo risorgimento fino al 1787. Preceduta da una teoria, ed istoria generale de' tremuoti*. Stamperia Regale, Napoli.

Wakita, H. (1975). Water wells as possible indicators of tectonic strain. *Science* 189, 553–555. doi:10.1126/science.189.4202.553

Wells, D.L., and Coppersmith, K.J. (1994). New empirical relationships among magnitude, rupture length, rupture width, rupture area, and surface displacement. *Bull. Seismol. Soc. Am.* 84, 974–1002.

Westaway, R. (1992). Seismic moment summation for historical earthquakes in Italy: Tectonic implications. *J. Geophys. Res.* 97, 15437–464. doi:10.1029/92jb00946